

CHARACTERIZATION OF PRIMARY NIOBIUM PARTICLES IN STAINLESS STEELS WITH DIFFERENT NICKEL CONTENTS

¹Anže BAJŽELJ, ¹Barbara ŠETINA BATIČ, ²Jožef MEDVED, ^{1,2}Jaka BURJA

¹*Institute of Metals and Technology, Ljubljana, Slovenia, EU, anze.bajzelj@imt.si, barbara.setina@imt.si, jaka.burja@imt.si*

²*University of Ljubljana, Faculty of Natural Sciences and Engineering, Department of Materials and Metallurgy, Ljubljana, Slovenia, EU, jozef.medved@ntf.uni-lj.si*

<https://doi.org/10.37904/metal.2022.4407>

Abstract

The presence of primary Nb-particles and their morphology affected by changes in nickel concentration in the as-cast microstructure of stainless steels with 18 wt% Cr were analysed. The formation of primary particles is due to the decreasing solubility during cooling and solidification of the steel melt, and additionally, segregation of alloying elements occurs during solidification, which contributes to the formation of particles. The coarse, sharp-edged nitrides formed during solidification reduce the mechanical properties of the material, highlighting a significant reduction in impact toughness and resistance to high temperature creep. According to the thermodynamic models the solubility of Nb and N was estimated. Solubility product of NbN decreases by lowering temperature and increasing the Ni content. With the Scheil-Gulliver model, it was predicted that, in a solution with (wt%) 18Cr, 0.5Nb and 0.03N precipitation of primary Nb-particles starts at solid fractions 0.91. The results were also confirmed using the Scheil solidification calculator with Thermo-Calc program. Three batches containing 9, 4.7 and 0.16 wt% Ni were prepared in an open induction furnace and cast into sand moulds. The presence of primary Nb-particles, eutectic phases and heterogeneous nucleation particles on MnS non-metallic inclusions were observed in the microstructure using an optical microscope and scanning electron microscope. By lowering the Ni content in the solution, the solubility product of NbN increases and the proportion of primary particles are lower. During cooling the solubility of Nb-particles decreases, small NbCN precipitate on grain boundaries and on MnS non-metallic inclusions.

Keywords: Stainless steel, niobium nitrides, niobium carbonitrides, solubility product, microsegregations

1. INTRODUCTION

Stainless steels are designed for use in more aggressive environments where corrosion resistance is required. A thin layer of chromium oxide forms on the surface of stainless steels, which protects the material from oxidation. Additionally, stainless steels can be alloyed with elements such as niobium, titanium, vanadium, etc. The main purpose of mentioned alloying elements is the formation of fine carbides, nitrides and other phases, thereby stabilizing the microstructure of stainless steels and improving their mechanical properties [1-6]. To improve the mechanical properties, the particles (carbides, nitrides) must be as small as possible and evenly distributed throughout the matrix, so the concentrations of these alloying elements are usually low. However, despite the low concentrations of alloying elements, segregation occurs during solidification and the formation of large, sharp-edged, primary particles in the interdendritic spaces. Primary particles do not dissolve completely during annealing, leading to local inhomogeneities in the chemical composition of the material. Due to their shape, large primary particles have a negative effect on mechanical properties, especially reducing impact toughness and high-temperature creep resistance, because the particles are poorly distributed, the movement of dislocations and crystal boundaries is easier [7-11].

The solubility of nitrogen and the solubility product of nitrides depend on the chemical composition of stainless steels. The influence of the elements in steel melt is determined by the interaction coefficients. In the present work, the influence of Ni-content in solution on the solubility of NbN product in stainless steels with 18 wt% Cr is studied. Nickel reduces the solubility of N in the steel melt, so the solubility product of niobium nitrides is expected to be lower at higher nickel contents [12-15].

2. MATERIALS AND METHODS

Three batches were prepared in an open induction furnace with the chemical compositions given in **Table 1**. A protective argon atmosphere was established above the steel melt surface to prevent oxidation of the melt. The melt was poured into a sand mould presented in **Figure 1** prepared by CO₂ process. The temperature of the steel melt was monitored with type B thermocouples (PtRh30 - PtRh6).

Table 1 Chemical compositions of as-cast samples in wt%

Sample	C	Si	Mn	S	Cr	Ni	Nb	N	Fe
10Ni	0.042	0.32	0.78	0.021	18.19	9.00	0.49	0.039	bal.
5Ni	0.035	0.24	0.77	0.014	18.70	4.70	0.45	0.040	bal.
0Ni	0.041	0.24	0.65	0.013	18.36	0.16	0.47	0.030	bal.

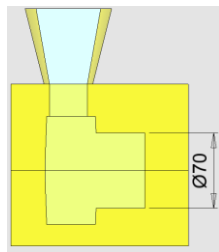


Figure 1 A side view drawing of the sand mould and casting

Samples for metallographic analysis were cut from the middle of the Ø70 section of the castings. The ground and polished samples were etched with Vilella's reagent, followed by microstructural characterization with an optical microscope (OM) Microphot FXA, Nikon (Nikon, Minato City, Japan) with a 3CCD video camera Hitachi HV-C20A (Hitachi, Ltd., Tokyo, Japan). Characterization of nitride particles were performed by a scanning electron microscope (SEM) Zeiss CrossBeam 550 (Carl Zeiss AG, Oberkochen, Germany), with an Octane Elite EDAX EDS microanalyzer (AMETEK, Inc., Berwyn, IL, USA) for energy dispersive X-ray spectroscopy (EDS). Thermodynamic calculations were performed with the commercial software Thermo-Calc (Thermo-Calc 2017a, Thermo-Calc Software AB, Stockholm, Sweden). The Thermo-Calc software TCFE8 Steels/Fe-alloys database was used to obtain the thermodynamic data for the calculations with Scheil Solidification Simulation calculator.

3. RESULTS AND DISCUSSION

3.1. Niobium nitrides solubility

Excessive nitrogen concentration leads to the formation of gaseous bubbles or the formation of nitrides. Equation (1) describes the formation of NbN between dissolved niobium [Nb] and nitrogen [N] [7].



$$\Delta G^{\circ}_{\text{NbN}} = -221,557.9 + 102.1 \cdot T \quad [\text{J/mol}] \quad (2)$$

The constant of the chemical reaction of niobium nitrides formation (K_{NbN}) can be written as equation (3):

$$K_{\text{NbN}} = \frac{a_{\text{NbN}}}{f_{\text{Nb}} \cdot [\text{wt\% Nb}] \cdot f_{\text{N}} \cdot [\text{wt\% N}]} \quad (3)$$

At equilibrium equation (4) can be written:

$$f_{\text{Nb}} \cdot f_{\text{N}} \cdot e^{\frac{-\Delta G^{\circ}_{\text{NbN}}}{R \cdot T}} = \frac{1}{[\text{wt\% Nb}] \cdot [\text{wt\% N}]} \quad (4)$$

a_{NbN} represents the activity of niobium nitrides, f_{Nb} is the activity coefficient of niobium, f_{N} is the activity coefficient of nitrogen, $[\text{wt\% Nb}]$ and $[\text{wt\% N}]$ are weight percent of dissolved Nb and N, respectively, R is the general gas constant, T is the temperature in Kelvin.

The solubility product of Nb and N was estimated using thermodynamic model for solubility calculations. The interaction parameters employed by Yang et al. [13] were accepted in the present study. The solubility product of Nb and N will be decreased with temperature as shown in **Figure 2**. At lower temperatures equilibrium solubility product of NbN is lower, making nitride formation more likely. **Figure 3** shows the effect of Cr and Ni addition on solubility product of Nb and N. Cr increases the solubility of NbN, on contrary the addition of Ni decreases the solubility product of NbN.

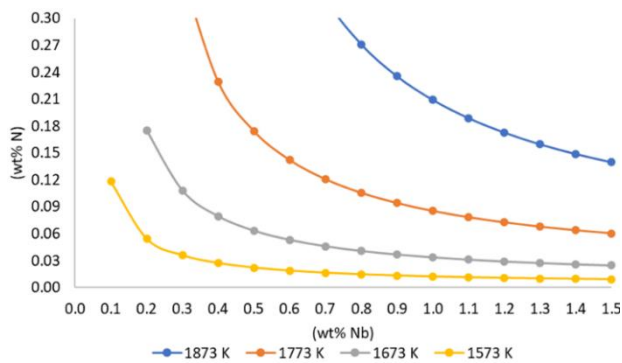


Figure 2 Effect of temperature on Nb and N solubility product in liquid steel melt

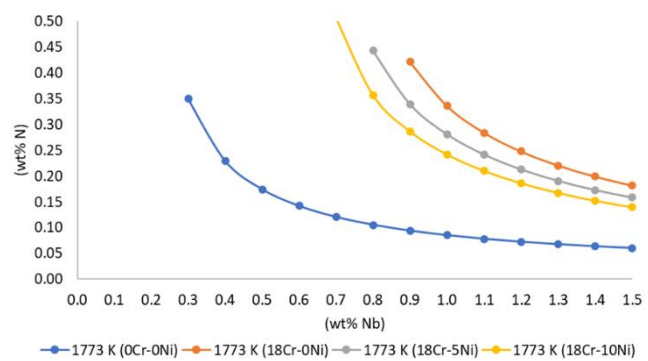


Figure 3 Effect of Cr and Ni content on Nb and N solubility product at 1773 K

3.2. Microsegregations of niobium and nitrogen

For the steel melt with 18 wt% Cr, 0.5 wt% Nb and 0.03 wt% N microsegregations were calculated according to Lever rule, Scheil-Gulliver, Brody-Flemings, Clyne-Kurz and Ohnaka microsegregations models. Local cooling rate (R_c), solidus temperature (T_s) and liquidus temperature (T_L) were set as 0.5 K/s, 1749 K and 1780 K, respectively, other data for the calculation were taken from references [8,9,16,17].

Figures 4 (a-c) show the relationship between the fraction solid and the concentration of niobium **(a)**, nitrogen **(b)** and the concentration product of niobium and nitrogen **(c)**, calculated by different models. The concentration increases the fastest according to the calculations of the Scheil-Gulliver model, which takes into account the complete diffusion of elements in the liquid phase and the non-diffusion state in the solid phase. The Lever rule assumes complete diffusion of elements in both the liquid and the solid phases, resulting in the slowest increase in element concentration. The other three models describe full diffusion in liquid and partial diffusion in solid phase. The equilibrium curve of the solubility product of niobium and nitrogen (green line) is plotted in **Figure 4c**, the area above the curve represents locally supersaturated solution and possibility for niobium nitrides formation. The equilibrium curve is intersected only in the case of calculations by the Scheil-Gulliver model at the end of solidification. With the Thermo-Calc program, equilibrium Scheil solidification calculations were performed, the results are given in the diagram in **Figure 4d**, and similarly show primary nitrides formation at the end of solidification cycle.

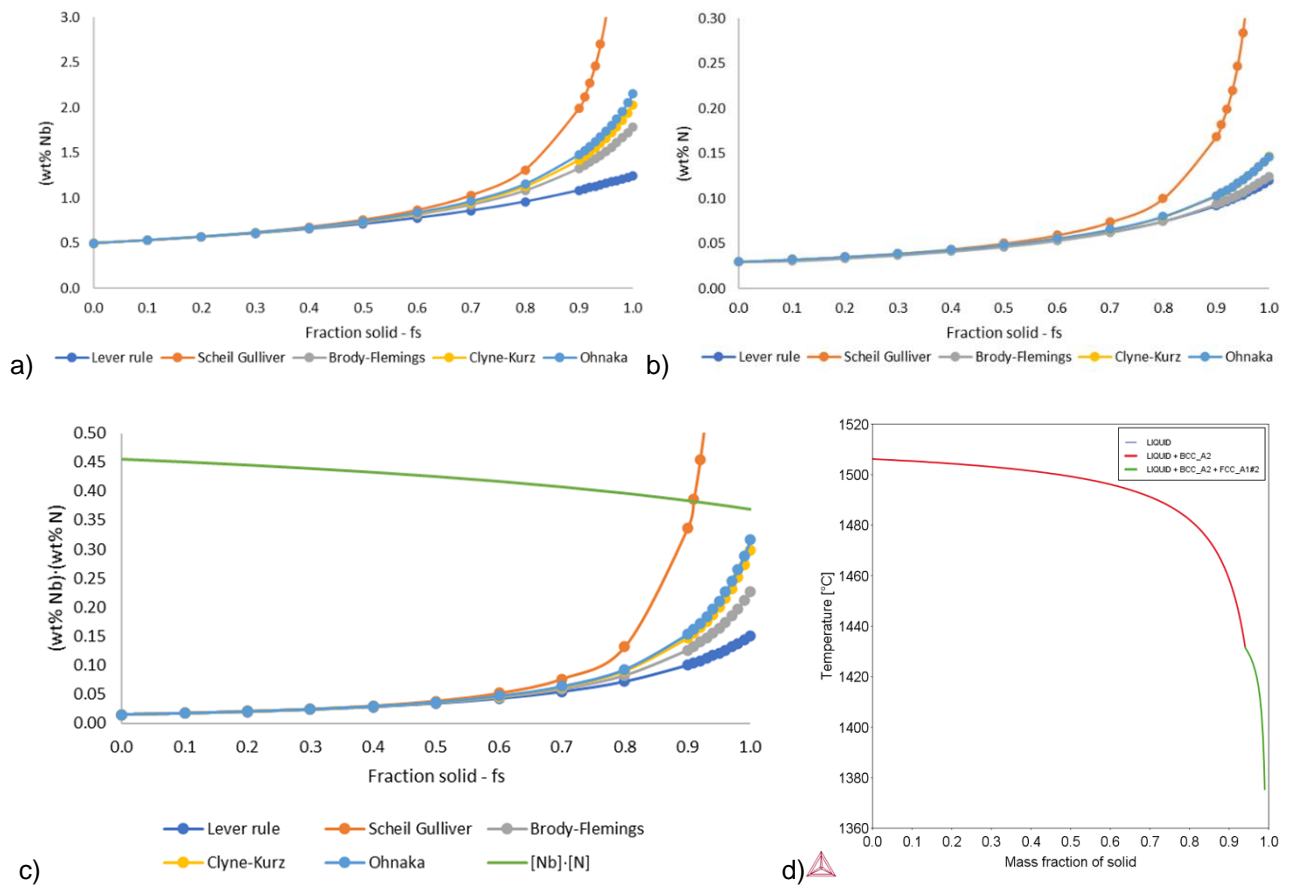


Figure 4 Concentrations of (a) Nb, (b) N, and (c) product of Nb and N at different fraction solid calculated by Lever rule, Scheil-Gulliver, Brody-Flemings, Clyne-Kurz and Ohnaka segregation models. (d) Scheil equilibrium solidification curve, calculated by using Thermo-Calc

3.3. Optical microscopy

Figure 5 shows optical microscopy images of etched as-cast samples. 10Ni sample has austenitic grains with traces of primary delta ferrite grains. 5Ni sample has austenite and ferrite grains, characteristic duplex stainless steels microstructure. With decreasing nickel content in the solution, the austenite range decreases, 0Ni sample has a ferritic microstructure.

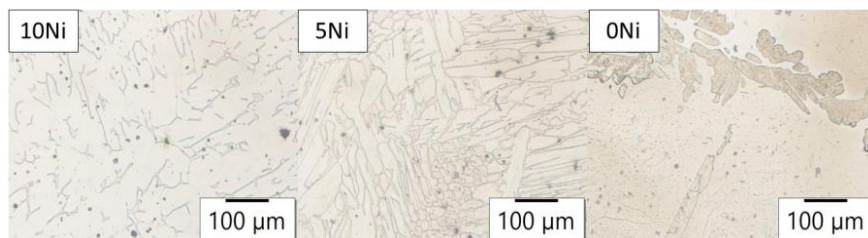


Figure 5 Optical microscopy of as-cast microstructures, etched with Vilella's reagent (SEM)

Figure 6 shows EDS elemental mapping of agglomerates of MnS non-metallic inclusions, primary Nb particles and eutectic phases in austenite matrix in 10Ni steel sample. The mapping images show that the primary Nb particles also contain C, indicating the formation of NbCN in the final solidification phase. In addition to NbCN, MnS non-metallic inclusions and eutectic phases ($\delta + \gamma + \text{NbCN}_{\text{prim}}$) were formed in the immediate vicinity at the end of the solidification. Light, thin layers of niobium carbonitrides were formed on MnS inclusions, which indicate formation of heterogeneously nucleated phase at the end of solidification.

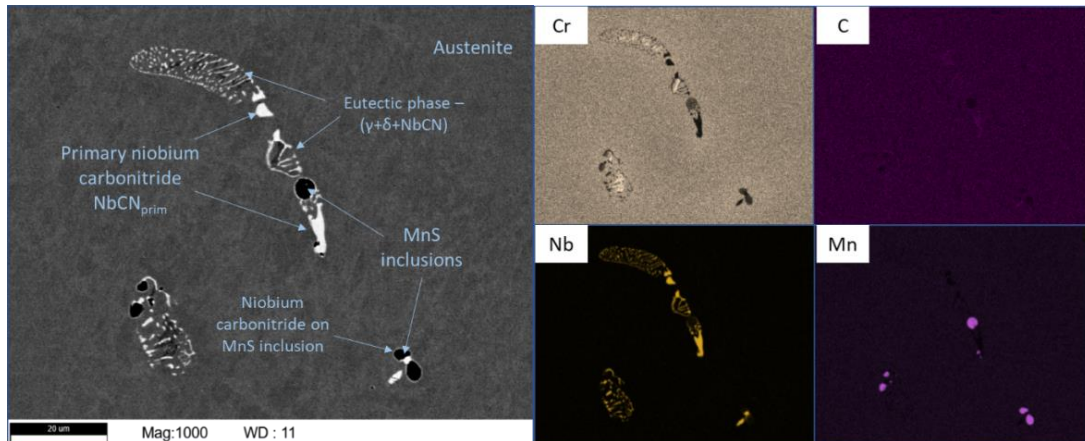


Figure 6 Backscattered electron image of MnS, NbCN and eutectic phase agglomerates in austenite matrix in 10Ni sample, and EDS elemental mapping of Cr, C, Nb and Mn

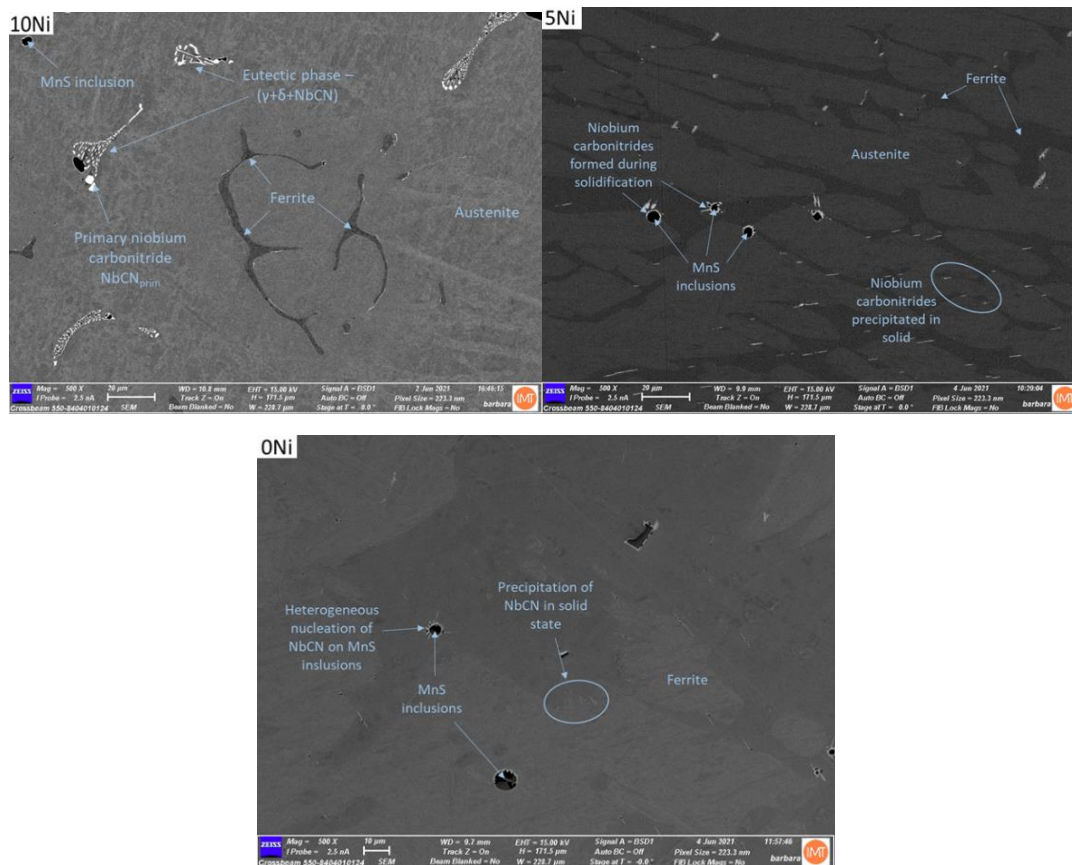


Figure 7 Backscattered electron images of 10Ni, 5Ni and 0Ni steel samples

Figure 7 shows backscattered electron images of 10Ni, 5Ni and 0Ni as-cast microstructure. In 10Ni steel sample darker areas represent untransformed delta ferrite, while the matrix are austenitic crystal grains. Between the austenite grain boundaries, where are the areas of microsegregations, MnS non-metallic inclusions, NbCN and eutectic phases precipitated during cooling. 5Ni steel sample contains ferrite grains (dark grey areas) and austenite crystal grains (light grey areas). MnS non-metallic inclusions and thin, white belt of NbCN formed during solidification, while needle-shaped NbCN along grain boundaries precipitated in solid. 0Ni steel sample contains MnS inclusions and heterogeneously nucleated layer on MnS of NbCN in ferrite matrix. Needle-shaped carbonitrides precipitated in solid state. With decreasing nickel content, the

formation of homogeneously nucleated primary NbCN and eutectic phases is negligibly small, the precipitation of NbCN is more pronounced in solid state.

4. CONCLUSION

The characterization of niobium particles in the as-cast microstructure of stainless steels with 18 wt% Cr and variable Ni-content was performed. It was shown that the solubility product of Nb and N decreases with decreasing temperature and Ni content, using thermodynamic models to calculate the solubility product. The drop in solubility product leads to the formation of NbCN. During solidification, local inhomogeneities in chemical composition due to segregation of alloying elements occur, the concentration of Nb and N in residual liquid during solidification was estimated using segregation models and the Thermo-Calc program.

Primary NbCN were characterized in segregation areas by scanning electron microscopy. Additionally, MnS non-metallic inclusions and eutectic phases were formed during solidification. Austenitic microstructure predominated in 10Ni steel samples, and agglomerates of MnS non-metallic inclusions, homogeneously nucleated primary NbCN, and eutectic phases were observed between the crystal grains. By lowering the Ni content in the solution, the proportion of carbonitrides formed during solidification was negligibly low, most Nb particles formed during cooling by forming needle-shaped particles around crystal boundaries and MnS non-metallic inclusions.

ACKNOWLEDGEMENTS

Funding was provided by the Slovenian Research Agency ARRS program P2-0050 (C).

REFERENCES

- [1] DAVIS, J. R. ASM Specialty Handbook Stainless Steels. Geauga County, OH, USA: ASM International, 1994.
- [2] DEARDO, A. J. Niobium in modern steels. *International Materials Reviews*. [online]. 2003, vol. 48, no. 6. pp. 371-402. Available from: <https://doi.org/10.1179/095066003225008833>.
- [3] GORDON, W., VAN BENNEKOM, A. Review of stabilisation of ferritic stainless steels. *Materials Science and Technology*. 1996, vol. 12, no. 2, pp. 126-131.
- [4] HIRAMATSU, N. Niobium in ferritic and martensitic stainless steels. In: *Proceedings of the International Symposium Niobium 2001*. Orlando, Florida, USA: 2002.
- [5] DULIEU, D. The role of niobium in austenitic and duplex stainless steels. In: *Proceedings of the International Symposium Niobium 2001*. Orlando, Florida, USA: 2002.
- [6] KEOWN, S. R., PICKERING, F. B. Niobium in stainless steels. In: *Proceedings of the International Symposium Niobium 81*. Warrendale, Pennsylvania, USA: American Institute of Mining, Metallurgical and Petroleum Engineers. 1984, pp. 1113.
- [7] BURJA, J., KOLEŽNIK, M., ŽUPERL, Š., KLANČNIK, G. Nitrogen and nitride non-metallic inclusions in steel. *Materiali in Tehnologije*. [online]. 2019, vol. 53, no. 6, pp. 919-928. Available from: <https://doi.org/10.17222/mit.2019.247>.
- [8] PENG QU, T., TIAN, J., LAI CHEN, K., XU, Z., YONG WANG, D. Precipitation behaviour of TiN in Nb-Ti containing alloyed steel during the solidification process. *Ironmaking and Steelmaking*. [online]. 2019, vol. 46, no. 4, pp. 353-358. Available from: <https://doi.org/10.1080/03019233.2017.1396722>.
- [9] YOU, D., MICHELIC, S. K., PRESOLY, P., LIU, J., BERNHARD, C. Modeling inclusion formation during solidification of steel: A review. *Metals*. [online]. 2017, vol. 7, no. 11. Available from: <https://doi.org/10.3390/met7110460>.
- [10] ZHANG, Y., LI, M., GODLEWSKI, L. A., ZINDEL, J. W., FENG, Q. Creep Behavior at 1273 K (1000 °C) in Nb-Bearing Austenitic Heat-Resistant Cast Steels Developed for Exhaust Component Applications. *Metallurgical and Materials Transactions A: Physical Metallurgy and Materials Science*. [online]. 2016, Vol. 47, No. 7, pp. 3289-3294. Available from: <https://doi.org/10.1007/s11661-016-3544-1>.

- [11] ZHANG, Y., YANG, J. Formation of Nb(C,N) carbonitride in cast austenitic heat-resistant steel during directional solidification under different withdraw rates. *Materials*. [online]. 2018, Vol. 11, No. 12. Available from: <https://doi.org/10.3390/ma11122397>.
- [12] SIGWORTH, ELLIOTT, J.F. The Thermodynamics of Liquid Dilute Iron Alloys. *Metal Science*. 1974, Vol. 8, No. 1, pp. 298-310.
- [13] YANG, S., LI, H., FENG, H., LI, X., JIANG, Z., HE, T. Nitrogen solubility in liquid Fe-Nb, Fe-Cr-Nb, Fe-Ni-Nb and Fe-Cr-Ni-Nb alloys. *ISIJ International*. [online]. 2021 Vol. 61, No. 5, pp. 1498-1505. Available from: <https://doi.org/10.2355/ISIJINTERNATIONAL.ISIJINT-2020-627>.
- [14] WAN-YI, K., CHANG-OH, L., CHUL-WOOK, Y., JONG-JIN, P. Effect of Chromium on Nitrogen Solubility in Liquid Fe-Cr Alloys Containing 30 mass% Cr. *ISIJ International*. 2009, Vol. 49, No. 11, pp. 1668-1672.
- [15] KOBAYASHI, Y., TODOROKI, H., SHIGA, N., ISHII, T. Solubility of nitrogen in Fe-Cr-Ni-Mo stainless steel under a 1 atm N₂ gas atmosphere. *ISIJ International*. [online]. 2012, Vol. 52, No. 9, pp. 1601-1606. Available from: <https://doi.org/10.2355/isijinternational.52.1601>.
- [16] CHOUDHARY, S. K., GHOSH, A. Mathematical Model for Prediction of Composition of Inclusions Formed during Solidification of Liquid Steel. *ISIJ International*. 2009, Vol. 49, No. 12, pp. 1819-1827.
- [17] YOU, D. Modeling microsegregation and nonmetallic inclusion formation based on thermodynamic databases. Leoben, 2016. Doctoral thesis. Montanuniversität Leoben.